

control system converges stably.

The control system is stable and converges when the first circumferential mode is generated in the duct. The control system is found to reduce the fan noise in the far field on an arc around the fan inlet by as much as 20 dB with none of the sound amplification associated with mode spillover.

INTRODUCTION

The emergence of the ultra-high bypass ratio engine on aircraft in the 21st century is expected to pose new and significant challenges to the noise control engineers. The dominant engine noise source will shift from the jet to the fan. The blade tip speed will be subsonic or transonic so that the fan noise will have high tonal content at harmonics of the blade passage frequency and the fundamental tone will be at a frequency less than 1000 Hz. In order to provide sufficient thrust, the engine diameter will be on the order of 3.66 meters (12 feet); and, in fact, engine size will be limited by considerations such as space available under the wing and allowable landing gear length. Weight is a significant parameter in the design of the power plant and in order to minimize the weight of the large diameter nacelle, it will be as short and as thin as possible. The relatively low blade passage frequency necessitates thick bulk liner treatment which is extensive in the axial direction, while thickness and length restrictions limit the amount of passive noise control treatment that can be applied.

The conflicting goals of minimum weight and maximum noise reduction can be aided materially by active noise control. Active noise control is well suited for applications in which a low frequency noise source limits the utility of passive control methods.¹ An active noise control system can provide significant noise reduction without excessive weight penalty, and research is continuing on development of light-weight, efficient control sound sources.²

Noise in ducts has long been considered an attractive application of active noise cancellation because the duct serves as a wave guide both to the source noise and to the control sound. Paul Lueg was issued a patent nearly 60 years ago for control of sound in a long duct using a system that consists of a reference microphone to measure the noise to be controlled, a source for the control sound which is equal in

is generated by a fan, and when the only frequency information about the control system described in this paper is an acoustic reference signal from a microphone on the fan.

Active noise control systems have been used to reduce multiple harmonic tones of periodic noise generated in a duct by a loudspeaker. Other researchers have demonstrated control of the sound generated by fans, either multiple tones,^{8,9} or broadband fan noise.⁵ Experiments reported generally show the noise reduction in an error microphone where the cancellation is attempted to be quite effective. Researchers at Virginia Polytechnic Institute and State University have developed an active control system on a commercial jet engine using a ring of microphones as the control source.¹⁰ The error microphones are located in the acoustic far field. Other experiments with this engine, have shown results so that the sound is effectively integrated over the finite space. The result is a broad band reduction of noise reduction with a slight loss of effectiveness. The most significant problem encountered in the experiment is the mode spillover due to the mode compositions of the noise and the control sources. This mode spillover results in sound amplification at some locations away from the microphones.

The purpose of the experiment reported in this paper is to develop a control system using microphones and sensors located in the fan duct. It is to determine the spatial extent of noise reduction and to determine, importantly, the mode spillover effect, can be controlled more effectively with the in-duct error microphone.

CONTROL THEORY

This section discusses the general theory of the development of the Least Mean Squares (LMS) Algorithm and the Adaptive Filter. A block diagram of the generalized control system is shown in figure 1. The block labeled "PLANT" represents the transfer function in which some mean value of the continuous signals is the input and the output is the disturbance signal d . The control system, represented by the dashed lines, generates a discrete signal u which combines with the disturbance signal to produce the error ϵ . It is the purpose of the control system to generate the signal which minimizes the error.

$$X_k = \begin{Bmatrix} x_k \\ x_{k-1} \\ \vdots \\ \vdots \\ x_{k-n+1} \end{Bmatrix}$$

The element x_k is the digitized sample of s taken at the present time. The element x_{k-1} is the digitized sample of s taken on the previous loop, Δ seconds in the past, and so on to x_{k-n+1} which is the digitized sample of s taken $(n-1)*\Delta$ seconds in the past. The vector X_k is constantly updated on each loop with the oldest value discarded, and the newest value put in the top of the array. The scalar output of the adaptive filter is obtained from :

$$(1) \quad y_k = \sum_{l=0}^{n-1} w_l x_{k-l} = W^T X_k$$

where:

W^T = the transpose of the vector W and
 W = a vector of weighting coefficients;

$$= \begin{Bmatrix} w_0 \\ w_1 \\ \vdots \\ \vdots \\ w_{n-1} \end{Bmatrix}$$

The error at time t_k is the combination of the disturbance and the filter output:

$$(2) \quad \epsilon = d - W^T X_k$$

The mean square error, ϵ^2 , is minimized by setting to zero the derivative of the expectation of the mean square error with respect to the weighting vector.¹¹ The LMS Algorithm is intended to approximate the optimum solution in real time, using the method of steepest descent. The weight function for the current loop through the controller, W_j is updated using the weight function from the previous pass through the loop, W_{j-1} plus a change proportional to the negative gradient of the mean square error, ∇_j

The weighting vector is updated in accordance with the expression:

$$(5) \quad W_j = W_{j-1} - 2\mu \nabla_j$$

$$= W_{j-1} - 2\mu \epsilon X_k$$

where:

μ = user defined adaptation coefficient

The algorithm will converge in the mean square sense as long as the adaptation coefficient is positive and less than the reciprocal of the largest eigenvalue of the matrix formed from the vector X_k and its transpose.¹¹ The value of μ which the algorithm converges is dependent on the adaptation coefficient and the convergence rate for the largest value of μ that does not cause instability. The maximum value criterion. The expected weight vector in expression 5 converges to the optimum Weiner weight vector when the input signals are uncorrelated over time.

MODAL DESCRIPTION OF SOUND IN DUCTS

The homogeneous wave equation for a sound wave of frequency ω traveling in a cylindrical duct of quiescent air is solved in order to determine the natural frequencies and mode shapes:

$$(6) \quad \frac{1}{r} \frac{\partial}{\partial r} \left(r \frac{\partial p}{\partial r} \right) + \frac{1}{r^2} \frac{\partial^2 p}{\partial \theta^2} + \frac{\partial^2 p}{\partial z^2} + k^2 p = 0$$

where:

$k = \frac{\omega}{c}$
 c = speed of sound
 r = the radial coordinate
 z = the axial coordinate
 θ = the circumferential coordinate

The solution of the wave equation has the following form:

$$(7) \quad p(r, \theta, z) = e^{ik_z z} \{ A_m J_m(k_{mn} r) \cos(m\theta) + i B_m Y_m(k_{mn} r) \sin(m\theta) \}$$

which $k < k_m$ are said to be cut on.

The plane wave is always present in the duct since it cuts on at 0 Hz. The first two spinning modes corresponding to the lowest order radial mode cut on at wave number normalized by the outer radius of the duct, $ka=1.84$ for the (1,0) mode and $ka=3.05$ for the (2,0) mode.¹² The zero order spinning mode associated with the first radial mode (0,1) cuts on at $ka=3.83$. These are the values expected for a duct with no centerbody.

The tonal part of the fan noise is generated by the impingement of the vortices shed from the rotor on the downstream fan exit guide vanes. These tones occur at the blade passage frequency and its harmonics. When the frequency is high enough that the wave can propagate, the fan tones travel in spinning modes defined from the relationship:¹²

$$(9) \quad m = n_h B + kV$$

where:

- n_h = harmonic number
- B = number of blades
- V = number of fan exit guide vanes
- k = any positive or negative integer, including zero

When the number of blades and the number of vanes is the same, the plane wave, $m=0$, is most strongly excited. When the difference in the number of blades and vanes is 1, the first spinning mode will dominate at frequencies above the $m=1$ cut-on. The spinning mode is characterized by a sound radiation deficit on the fan axis. The sound is in a lobe which radiates perpendicular to the duct axis when the mode is first cut on and progresses toward the duct axis as the frequency increases.¹³

EXPERIMENT LAYOUT

Duct

The experimental setup consists of a duct with the following major elements: inflow control device, control hardware section, an axial flow fan, and an anechoic termination. The unit is installed in the laboratory space of the Anechoic Noise Facility at

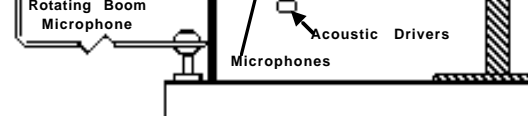


FIGURE 2. Fan noise control experiment.

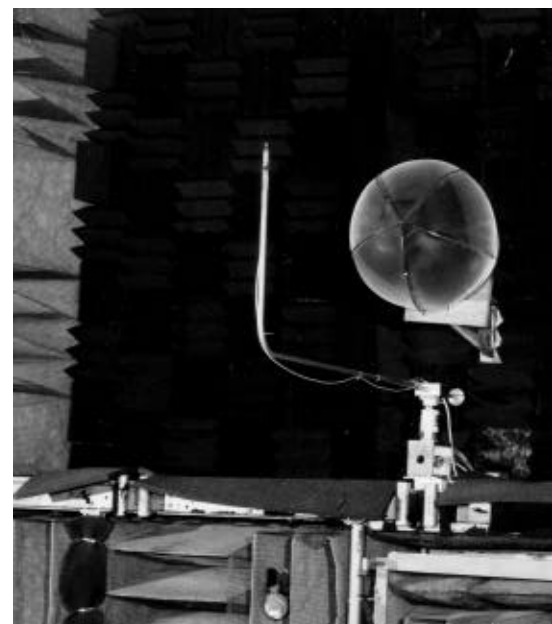


FIGURE 3. Fan noise control duct inside the anechoic chamber. The inflow control device and the microphone are visible.

The control hardware duct piece contains 24 microphones arranged uniformly around the duct and installed flush with the duct wall. The error sensors in the duct are taken from among these 24 microphones. The error sensors are 3.2 mm (1/8 inch) diameter transducers embedded in a threaded (1/2 inch) diameter canister. Twelve drivers are distributed around the duct, as shown in the photograph, figure 4. Each driver is a 100 W rms. The drivers are attached to the duct through transition horns that are thick-walled to prevent sound transmission. The horns transition from the round outlet of the driver to the rectangular duct wall. The areas of both are



FIGURE 4. Fan noise control ductwork, view from outside the Anechoic Chamber showing noise control hardware, fan, and anechoic termination duct sections.

(11.81 inch) with a hub diameter of 15.2 cm (6 inch). The fan is driven by a 3 HP electric motor and rotor speeds up to 6000 rpm can be achieved. The blade passage frequency can thus be up to 1600 Hz. This frequency corresponds to wavenumber normalized by duct radius, $ka = 4.38$ for the 30 cm diameter duct. It is expected that the first two spinning modes of the lowest radial and the first radial mode associated with the zero order spinning mode will be cut on when the fan runs at 6000 rpm. No other higher order modes are expected to be cut on. The fan has been designed so that the number of stator vanes can be 16, 17, or 18 and always uniformly spaced. It is expected that the plane wave will dominate when the fan is configured with 16 stator vanes, the 1st circumferential (spinning) mode will dominate when 17 vanes are installed, and the 2nd circumferential (spinning) mode will dominate with the 18 vane configuration.

A muffler section is located downstream of the fan as shown schematically in figure 2 and in the photograph, figure 4. This 3.7 m (12 foot) long duct is lined with perforated metal and 50 mm (2 inch) of sound absorbing material. The muffler reduces fan noise radiation into the laboratory space and acts as an anechoic termination for the discharge of the fan.

Control System

The active, adaptive noise control system uses a time domain LMS algorithm. Figure 5 shows the

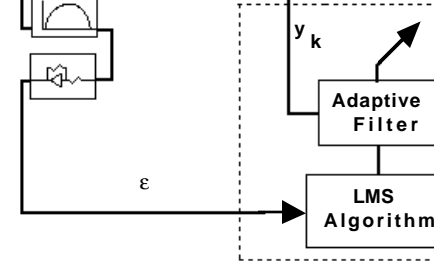


FIGURE 5. Fan noise control system block diagram.

The controller is a Texas Instruments (C30) floating point Digital Signal Processor board which is mounted in a personal computer through the ISA bus. The reference signals are input to the computer by a 16-bit Digital-to-Analog Converter with a fourth order anti-aliasing filter. The Analog-to-Digital Converter has a 153-KHz throughput. The signal is then processed by a 16-bit Digital-to-Analog Converter with a fourth order anti-aliasing filter to reconstruct and smooth the signal produced by the C30. The Digital-to-Analog Converter has a 667-KHz throughput.

The control algorithm consists of a 4th order Adaptive Filter which applies the reference signal to generate the control signal and a Least Mean Square algorithm which updates the weighting coefficients using the reference signal, the coefficients and the error. The adaptive control system is driven at the reference frequency (Δ) of the Analog-to-Digital Converter.

RESULTS

1. Plane Wave Generated in the Duct

A series of tests was run with the active noise control system incorporated in the duct system. The number of stator vanes was varied for these tests in order to excite plane waves. The rotor/stator spacing is set to a minimum value for the greatest rotor/stator interaction. The signals from two microphones at opposite circumferential locations in the duct are added in phase to measure the error signal. The control speakers are activated in phase to cancel the plane wave.

Figure 6 shows the directivity plot of the acoustic far field with the fan operating at 6000 rpm.

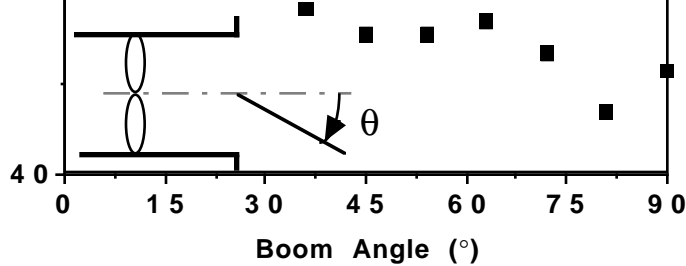


FIGURE 6. Far field directivity of BPF tone at fan speed 2350 rpm , plane wave dominant.

● : control off, ■ : control on

The fan was then run at 2800 rpm , which corresponds to blade passage frequency of 750 Hz or normalized wavenumber $ka=2.10$. This frequency is above the first spinning mode cut-on frequency for the duct, but it is expected that the spinning mode would not be cut on strongly in light of the fact that the number of blades and stators is the same. This is seen in the directivity plots of the blade passage frequency tones for control off and control on that are shown in figure 7. The far field sound is not as uniform spatially as it was below the mode cut-on, figure 6, indicating the presence of a higher order mode. However, the sound deficit on the fan axis that is characteristic of the spinning mode dominance is not found in the radiation pattern in figure 7, which indicates plane wave dominance. When the controller is activated, the sound level reduction is relatively uniform at 2 dB in the acoustic far field at locations from the fan axis to 90° . The far field noise reduction, while stable and spatially uniform, is much less than it is when blade passage frequency is below the spinning mode cut-on.

The performance of the controller as a function of frequency is indicated in figure 8. This plot was generated by operating the fan at speeds from 1500 rpm to 6000 rpm and comparing the blade passage frequency tones at the error microphone for control off with control on at each speed. The control off spectrum for the in-duct error microphone shows a general trend in sound level to go up with engine speed punctuated by increases at 2300, 3700, and 4800 rpm. The increases indicate the presence of standing waves in the duct. The 2300 rpm speed is

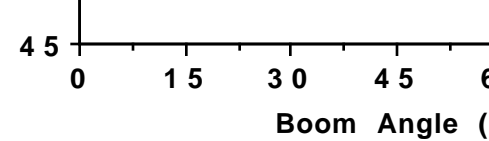


FIGURE 7. Far field directivity of BPF tone at fan speed 2800 rpm , plane wave dominant.

● : control off, ■ : control on

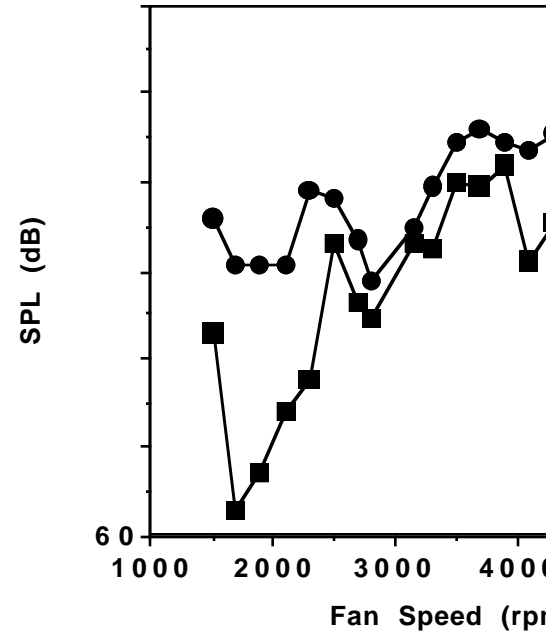


FIGURE 8. Sound level spectrum of blade passage frequency tones at the in-duct error microphone.

● : control off, ■ : control on

Figure 9 shows the spectral noise reduction in the far field on the axis of the duct. When control is off, the far field spectrum shows a peak at 2300 rpm. When control is on, it is in the duct, showing that the duct modes are not propagated into the far field. The noise reduction is obtained with the controller at all operating speeds except 2700, 3900, and 4800 rpm. These critical fan speeds are near the frequencies of the in-duct error microphones registered in the duct. Comparison of figures 8 and 9 shows that the noise reduction in the far field is

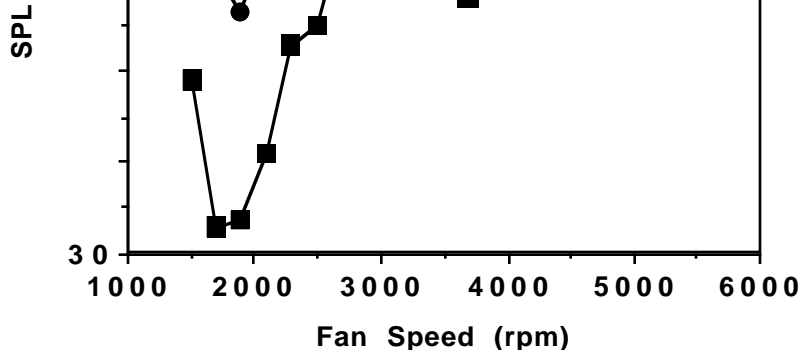


FIGURE 9. Sound level spectrum of fan BPF tone at far field microphone fixed on the duct axis, $\theta = 0^\circ$.

● : control off, ■ : control on

The fan was operated at 2800 rpm, which speed produces normalized wavenumber $ka = 2.10$. This is above the first spinning mode cut-on and it is expected that the $m=1$ spinning mode will be excited into dominance. This is shown in the far field radiation pattern, the lower curve in figure 10. The upper curve in figure 10 shows directivity of the experimental simulation produced by the control drivers at 750 Hz. The far field radiation pattern generated by the control drivers is seen to be comparable to the fan noise radiation.

The result of activating the control system is shown in figure 11. The spinning mode is virtually eliminated, leaving a radiation pattern that suggests a plane wave. This is reasonable since the plane wave is always generated by the fan and the control system is not programmed to reduce it.

CONCLUSIONS

The experiments discussed in this paper have verified that time domain active, adaptive control is applicable to reduction of fan noise in a duct. The control system has been applied to tones that are generated at the blade passage frequency. The controller is stable over a range of frequencies in which plane waves and higher order duct modes can propagate. The system utilizes in-duct error sensing which is shown to provide global noise reduction in the acoustic far field.

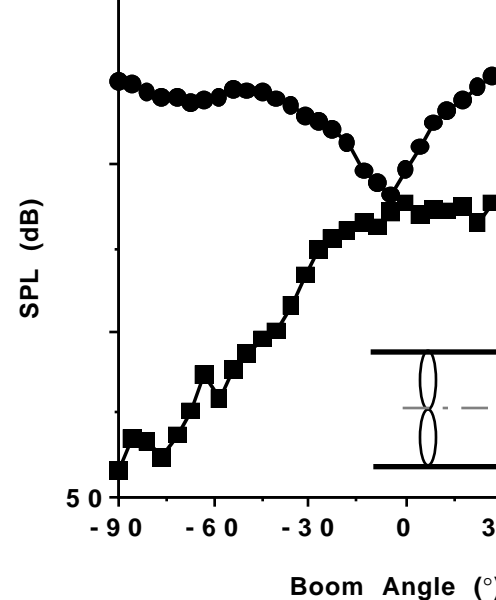


FIGURE 11. Far field directivity of fan BPF tone at fan speed 2800 rpm. $m=1$ mode dominant.

● : control off, ■ : control on

The system is most effective when the structures of the noise source and of the control source are the same. When the fan has an equal number of rotor blades and stator vanes, and the control drivers are configured to generate plane waves, far field noise reduction is greater than the cut-on of higher order modes. The plane wave modes, even though the plane wave is dominant, compromises noise reduction. When the number of stator vanes and rotor blades differs by 1, and the control drivers are configured to generate the $m=1$ mode, the control system reduces the first spinning mode, leaving the plane wave component which is inevitably generated by the rotor/stator interaction. The in-duct error sensing produces a stable control signal which reduces the uncontrolled higher order modes.

Generally the noise reduction measured in the error sensors is greater than the noise reduction in the far field. Fan operating conditions were chosen which the in-duct error sensor indicated a strong tone but no noise reduction was measured in the far field. In some instances the sound pressure level was increased with the control system.

5. Eriksson, L.J., Allie, M.C., Bremigan, C.D., and Gilbert, 1989, J.A., "Active Noise Control on Systems with Time-Varying Sources and Parameters", Sound and Vibration, vol. 23, no. 7, pp. 16-21.
6. Eghtesadi, K. and Chaplin, G.B., 1987, "The Cancellation of Repetitive Noise and Vibration by Active Methods", proceedings of NOISE-CON '87, State College, Pennsylvania, pp. 347-352.
13. Rice, E.J., 1978, "Multimodal Fan Noise Radiation Using Mode Cutoff Radiation", Journal, vol. 16, pp. 906-911.
14. Homyak, L., McArdle, J.G., and others, 1983, "A Compact Inflow Control System for Simulating Flight Fan Noise", J. of Sound and Vibration, vol. 93, no. 83-0680.
15. Chestnutt, D. ed., 1982, "Flight Fan Noise", NASA CP-2242.

